Turkish Journal of Electrical Engineering & Computer Sciences

http://journals.tubitak.gov.tr/elektrik/

Research Article

Turk J Elec Eng & Comp Sci
(2014) 22: 1298 – 1306

doi:10.3906/elk-1211-130

# Real-time control of an automated guided vehicle using a continuous mode of sliding mode control

**Birol SOYSAL***
Department of Electrical and Electronics Engineering, Ataturk University, Erzurum, Turkey

**Received:** 23.11.2012 • **Accepted:** 04.02.2013 • **Published Online:** 15.08.2014 • **Printed:** 12.09.2014

**Abstract:** This paper proposes a tracking control method for a certain type of differential-drive wheeled mobile robot, called automated guided vehicles (AGVs), using a continuous mode approach of sliding mode control (SMC). The SMC applied produces a continuous signal in between the U and –U control signals instead of discrete ones. The controller is applied to control the velocity and direction angle of the vehicle in order to keep it on a desired path. The obtained algorithm is applied to the experimental system under load and disturbance to show its robustness. The experimental results are satisfactory and verify the performance of the control algorithm.

**Key words:** Automated guided vehicle, trajectory tracking, sliding mode control

## 1. Introduction

The automated guided vehicle (AGV) was recently used in various applications, such as transportation, planetary exploration, mining, and military operations. As AGVs have been increasingly used in a wide range of applications, research in this area has attracted considerable attention over the past 2 decades. At the beginning, to achieve accurate motion control, the designed controllers in most of the research were only based on a kinematic model of the AGV [1–3]. However, in real-time applications, it is difficult to obtain a satisfied tracking performance when only considering a kinematic model, when high-speed motion or heavy-load transportations are required. Therefore, it becomes essential to consider the robot's dynamics and its kinematics at the same time.

As a solution, several nonlinear techniques have been used to integrate the dynamic controller with a kinematic controller in recent years. Fuzzy-net control [4–6], neural control [7–9], dynamic feedback linearization [10], back-stepping control [11–13], and adaptive control [14,15] have been used to solve trajectory-tracking and robust control problems of AGV. Sliding mode control (SMC) has gained much attraction for machine control applications [16,17]. SMC is a very effective approach for the solution of the problem due to its robustness to parameter variations, easy implementation, fast dynamic response, and disturbance rejection [18]. A comprehensive review of SMC was presented in [19–21]. It has been widely reported that SMC exhibits unwanted motion, called chattering. This chattering is caused due to discontinuity of the control actions.

In this paper, a continuous mode of SMC (CMSMC) is applied to the experimental setup of an AGV. The actuator dynamics with 2 wheels of the AGV are included in the system model. The experimental results obtained demonstrate that the controller is robust to load changes and disturbances, and can follow command trajectories very well.

*Correspondence: bsoysal@atauni.edu.tr

## 2. Design of the AGV

The differentially-driven AGV considered in this paper is depicted in Figure 1. It consists of a mobile platform with 2 differential driving wheels mounted on the same axis and a rear free wheel to keep the platform stable. The motion and orientation are achieved by independent actuators of the left and right wheels, e.g., DC motors providing the necessary torques to the front wheels.

We can write the following kinematic differential equations from the motion equations of the vehicle [22]:

$$v_R = R \cdot \omega_R, \tag{1}$$

$$v_L = R \cdot \omega_L, \tag{2}$$

$$v = \frac{v_R + v_L}{2} = \frac{R}{2} \quad (\omega_R + \omega_L), \tag{3}$$

$$\frac{d\phi}{dt} = \frac{R}{L} \quad (\omega_R - \omega_L), \tag{4}$$

$$\frac{dx}{dt} = v_x = v \cdot \cos \ (\ \phi) = \frac{R}{2} \ (\ \omega_R + \omega_L) \cos \ (\phi) \ , \tag{5}$$

$$\frac{dy}{dt} = v_y = v \cdot \sin \ (\ \phi) = \frac{R}{2} \ (\ \omega_R + \omega_L) \sin \ (\phi) \ , \tag{6}$$

where $L$ is the distance between the wheels and $R$ is the radius of the wheel. $v_R$ and $v_L$ represent the linear velocities of the right and left wheels, $\omega_R$ and $\omega_L$ are the angular velocities of the right and left wheels, and $v$ and $\phi$ are the vehicle linear velocity and the vehicle direction angle, respectively. $v_x$ is velocity component in the $x$ direction and $v_y$ is the velocity component in the $y$ direction. The vehicle has 2 wheels on the front, and each of the front wheels is independent and driven by a separately excited DC motor, through a gear box; Figure 2 shows the simplified drive system.

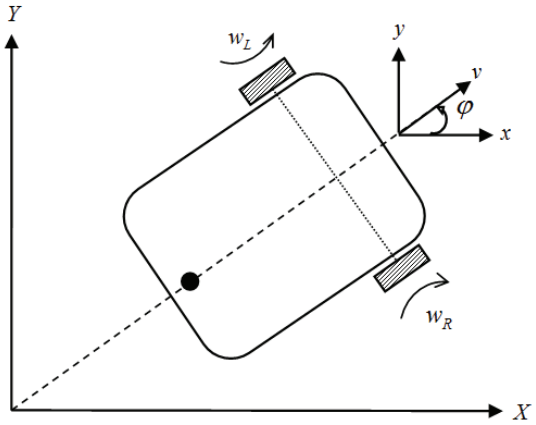


**Figure 1.** Vehicle model and its coordinate system.

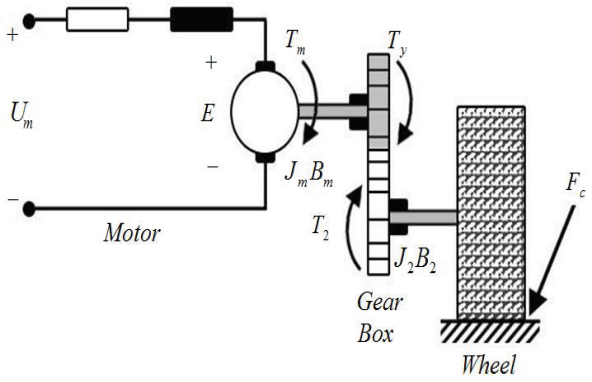


**Figure 2.** Drive system for each wheel of the vehicle.

The torque transferred from the motor to the gearbox can be written as follows:

$$T_m = J_m \frac{d^2\theta_m}{dt^2} + B_m \frac{d\theta_m}{dt} + T_{Load}, \tag{7}$$

$$T_{Load} = n^2 J_2 \frac{d^2\theta_m}{dt^2} + n^2 B_2 \frac{d\theta_m}{dt} + nF_c \frac{\dot{\theta}_m}{\left|\dot{\theta}_m\right|}, \tag{8}$$

where $J_m$ is the inertia, $B_m$ is the friction coefficient, $\theta_m$ is the angle of rotation, $n$ is the reduction ratio of the gearbox, and $F_c$ is the Coulomb torque constant. From Eqs. (7) and (8):

$$T_m = (J_m + n^2 J_2)\frac{d^2\theta_m}{dt^2} + (B_m + n^2 B_2)\frac{d\theta}{dt} + nF_c sign(\dot{\theta}_m), \tag{9}$$

$$\eta_1 = \frac{B_m + n^2 B_2}{J_m + n^2 J_2}, \quad \eta_2 = \frac{nF_c}{J_m + n^2 J_2}, \quad \eta_3 = \frac{1}{J_m + n^2 J_2}, \tag{10}$$

$$\frac{d^2\theta_m}{dt^2} = -\eta_1 \frac{d\theta_m}{dt} - \eta_2 sign(\dot{\theta}_m) + \eta_3 T_m). \tag{11}$$

To represent the vehicle equation in the state space, we select the state vector as:

$$v = \frac{v_R + v_L}{2} = \frac{R}{2} \quad (\omega_R + \omega_L) \quad x_2 = \dot{\theta} \quad x_3 = \theta. \tag{12}$$

Next, the above equations, which describe the dynamics of the vehicle, can be written in a more convenient matrix form as:

$$v = \frac{v_R + v_L}{2} = \frac{R}{2} \quad (\omega_R + \omega_L), \tag{13}$$

where

$$v = \frac{v_R + v_L}{2} = \frac{R}{2} \quad (\omega_R + \omega_L) \quad g_2(x) = \frac{1}{2}x_1 - \frac{1}{2R}x_2. \tag{14}$$

Thus, our system can be shown in the nonlinear matrix form as:

$$\frac{dx}{dt} = f(x) + B(u), \tag{15}$$

where $u = [T_R \; T_L]^T$, $f(x)$, and $B$ are the matrices in Eq. (13).

## 3. The CMSMC

In general, a sliding surface ($\varepsilon$ ) is selected as shown below [21,22]:

$$\varepsilon(x,t) = G(x^r(t) - x(t)) = Ge = \emptyset(t) - \varepsilon_a(x), \tag{16}$$

where $\emptyset(t) = Gx^r(t)$, $\varepsilon_a(x) = Gx(t)$, and $x^r$ are the reference state vectors and $G$ is the slope matrix of the sliding surface. To provide the Lyapunov stability criteria, the candidate Lyapunov function is selected as:

$$V = \frac{1}{2}\varepsilon^T \varepsilon, \tag{17}$$

which is positive definite, and for the stability its derivative needs to be negative definite. This can be assured if the time derivative of the Lyapunov function can be expressed as:

$$\dot{V} = -\varepsilon^T D sign(\varepsilon) < 0, \tag{18}$$

where $D$ is a positive-definite matrix. Taking the derivative of Eq. (17) and equating it to Eq. (18), the following equation is obtained:

$$-\varepsilon^T D sign\,(\varepsilon) = \varepsilon^T \dot{\varepsilon}. \tag{19}$$

Using the plant equation, the expression for the derivative of the sliding function is obtained as:

$$\frac{d\varepsilon}{dt} = \frac{d\emptyset}{dt} - \frac{\partial \varepsilon_a}{\partial x}\frac{dx}{dt} = \frac{d\emptyset}{dt} - G(f\,(x) + Bu\,). \tag{20}$$

By putting Eq. (20) into Eq. (19), the control input to the system can be found as:

$$u(t) = u_{eq}(t) + (GB)^{-1} D sign\varepsilon, \tag{21}$$

where

$$u_{eq}(t) = (GB)^{-1}\left(\frac{d\emptyset}{dt} - Gf\,(x)\right). \tag{22}$$

Using Eqs. (20) and (22), the derivative of the sliding function can also be written as:

$$\frac{d\varepsilon}{dt} = GB(u_{eq} - u). \tag{23}$$

The equivalent control can be written in a different form, as given below:

$$u_{eq}(t) = u\,(t) + (GB)^{-1}\frac{d\varepsilon}{dt}, \tag{24}$$

where $u\,(t)$ does not change very much in a short time. For this reason, $u\,(t - \Delta t)$ can be used instead of $u\,(t)$. The estimation for equivalent control can be shown as:

$$u_{eq}(t) = u\,(t - \Delta t) + (GB)^{-1}\frac{d\varepsilon}{dt}. \tag{25}$$

By putting Eq. (25) into Eq. (21), the last form of the controller can be obtained as:

$$u(t) = u\,(t - \Delta t) + (GB)^{-1}(Dsign\varepsilon + \frac{d\varepsilon}{dt}). \tag{26}$$

It is well known that sliding mode techniques generate undesirable chattering that can be eliminated by replacing the switching function with a continuous one in the sliding surface neighborhood, that is:

$$\text{sign}(\varepsilon) = \begin{cases} 1 & if \quad \varepsilon > \rho \\ -1 & if \varepsilon < -\rho \\ \varepsilon/\rho & if \quad |\varepsilon| < \rho \end{cases} \quad \text{where}\, \rho > 0, \tag{27}$$

and further simplification can be introduced by replacing $d\varepsilon/dt$ with its first-order approximation in the discrete time version:

$$\frac{d\varepsilon}{dt} = \frac{\varepsilon\,(k) - \varepsilon(k-1)}{T}. \tag{28}$$

Next, under these conditions, Eq. (26) can be expressed for arbitrary $[-\rho\rho]$ as:

$$u(k+1) = u(k) + \frac{(GB)^{-1}}{T}[TD\varepsilon(k) + \varepsilon(k) - \varepsilon(k-1)]. \tag{29}$$

The block diagram of the vehicle control system is shown in Figure 3, where $v$ is the velocity and $\phi$ is the direction angle response of the AGV. The control of the AGV is based on the control of the velocity and direction angle. The controller uses the actual velocity, actual angle, and their reference values.

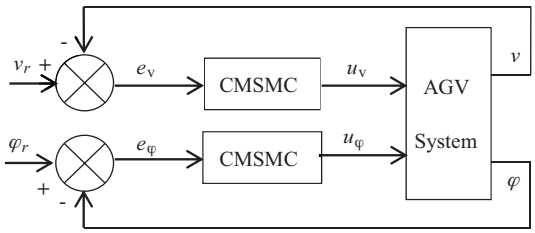


**Figure 3.** Block diagram of the vehicle control system.

## 4. Experimental results

Velocity and direction angle control of the AGV is performed in order to validate the effectiveness of the proposed CMSMC. The controller is applied on the AGV, which is shown in Figure 4, and developed in the Automatic Control Laboratory to prove the algorithm experimentally. Its weight is 17 kg under load. It is equipped with 2 fast-response servo motors with incremental encoders counting 500 pulses/turn, speed reduction gear boxes, an encoder interface card, a PC-DAQ, and analog motor driver circuits. The controller software is run on a 3.0-GHz Pentium IV, using Windows as a real-time operating system, with online implementation of the CMSMC.

**Figure 4.** Laboratory experimental vehicle.

To validate the proposed controller, many experiments are conducted. Experimental results of the vehicle system are shown in Figures 5–8. In the first experiment, the performance of the controller is tested for the

references of a sinusoidal velocity and sinusoidal direction angle under a 17-kg load. The measured and reference values of the velocity and direction angle, as well as errors of the velocity and direction angle, motor commands, and trajectories, are presented in Figure 5. It can be observed that the measured velocity and direction angle converge to the given references rapidly, the velocity and direction angle errors are profoundly reduced, the reference and measured trajectories are almost the same, and additionally, the produced actuator commands applied to the motor are continuous.

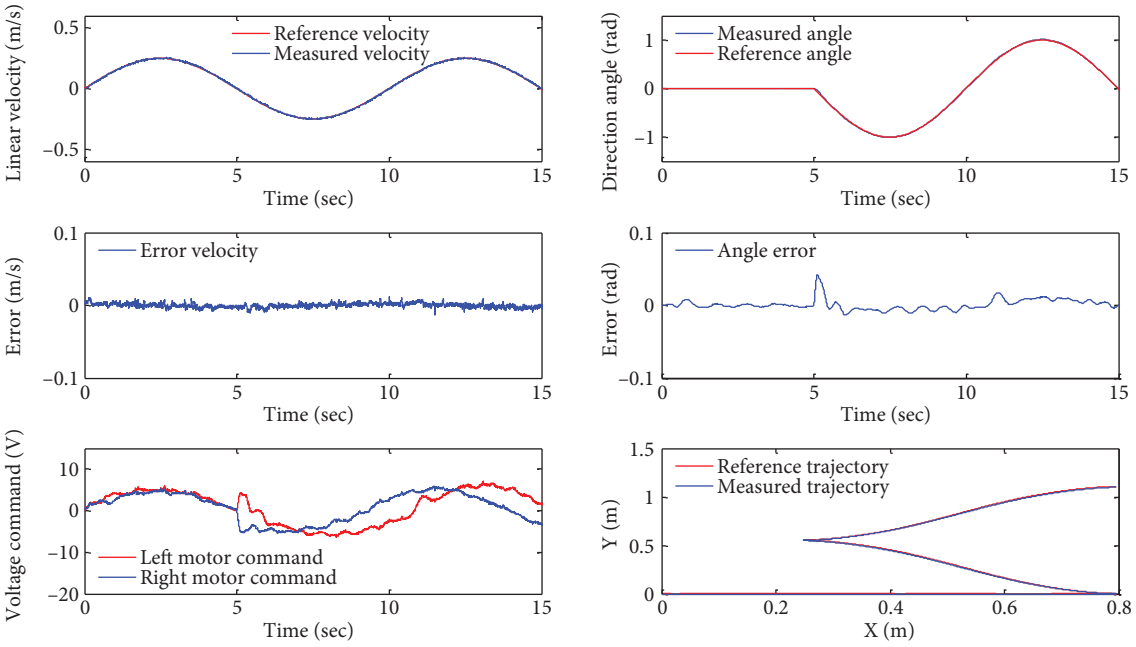


**Figure 5.** Experimental results for sinusoidal references under the 17 kg load.

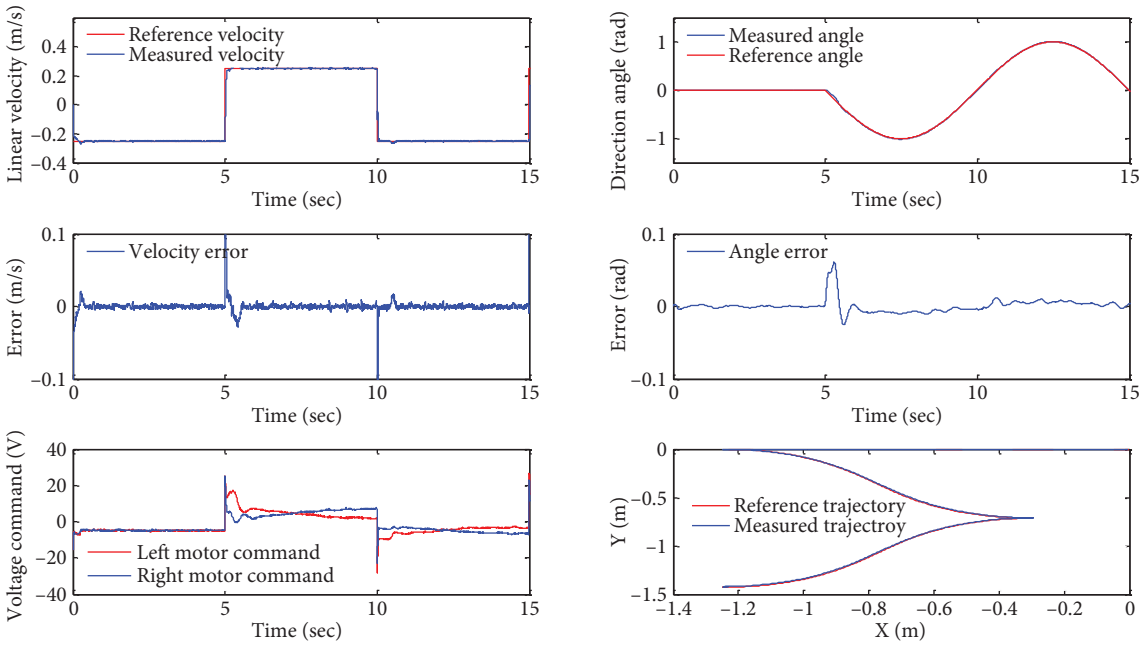


**Figure 6.** Experimental results for the square-wave and sinusoidal references under the 17 kg load.

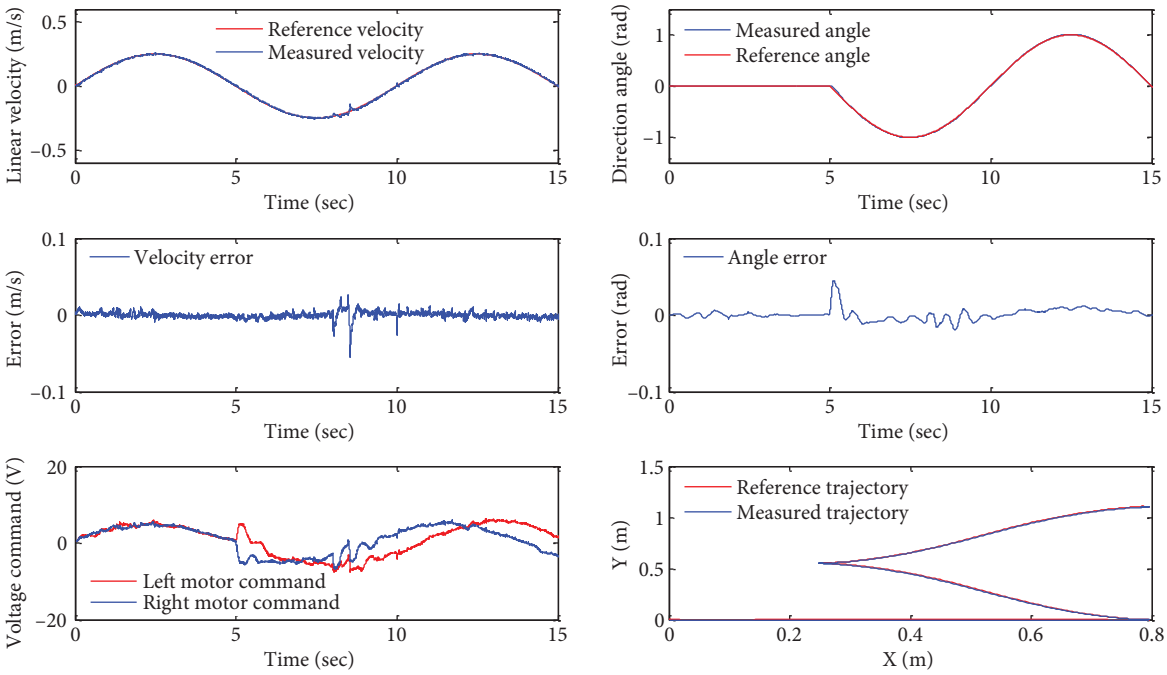


**Figure 7.** Experimental results for sinusoidal references under the 17 kg load and instant disturbance.

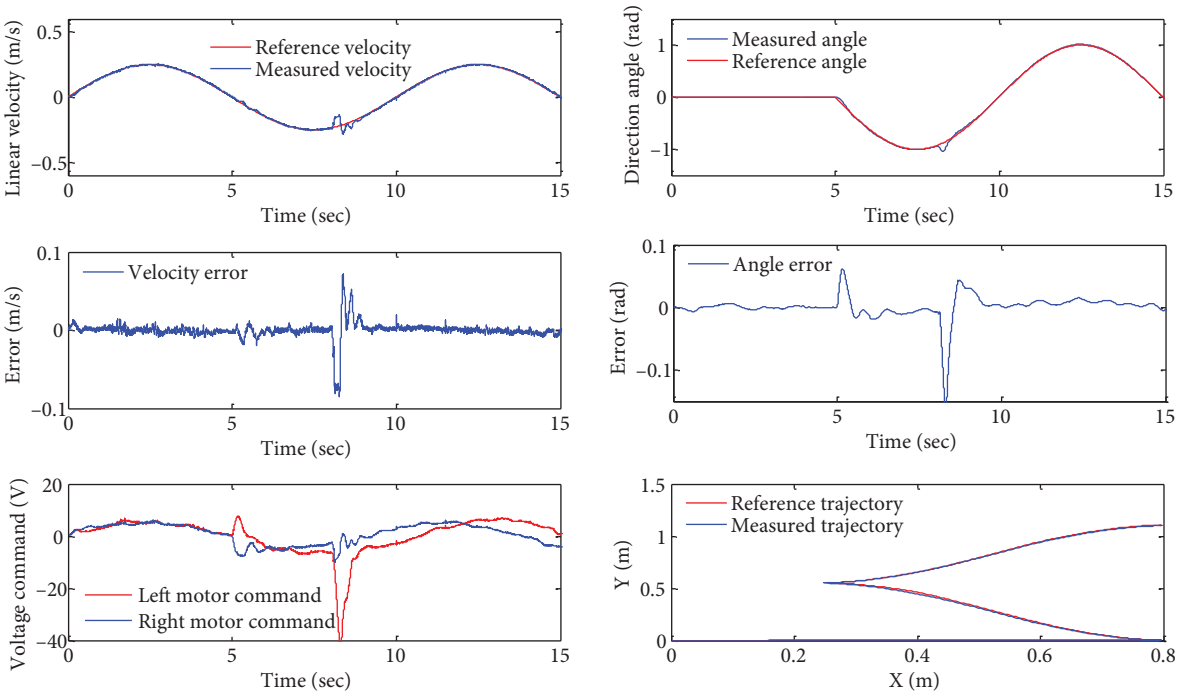


**Figure 8.** Experimental results for sinusoidal references under the 30 kg load and instant disturbance.

In the second case, a square-wave reference for the velocity is chosen. The square-wave reference is important to test the performance of the control algorithm for step changes. Figure 6 demonstrates that the proposed controller provides accurate tracking of the velocity and direction angle references. Both the reference and actual trajectories are very close to each other.

Finally, the controller is tested for an instant disturbance under the total loads of 17 kg and 30 kg, as shown in Figures 7 and 8, respectively. Instant disturbances are applied at approximately 7 s in Figures 7 and 8. Moreover, it is shown in Figure 8 that the response of the proposed controller is good enough under both the heavy load of 30 kg and instant disturbance. Furthermore, the controller adapts itself to the deteriorating conditions to overcome the disturbance quickly and follows the reference perfectly, as shown in the graphs of the voltage commands in Figures 7 and 8. It is also observed that the actuator commands have some oscillations because the AGV is run on a rough surface. The peaks in the command voltage and errors at 5 s, in all of the figures, originate from the change in the direction angle reference. It should be noted that the same peaks in Figure 6 are also due to both velocity and direction angle changes.

## 5. Conclusion

A continuous mode approach of SMC is applied to an AGV with complex references, instant disturbance, and extra load. The experimental results show that the proposed controller adapts itself to the changed conditions and can respond quickly to control the actual velocity and direction angle of the vehicle system. It is observed in all cases that the proposed controller provides good tracking performance and produces continuous actuator commands.

## Acknowledgments

The author would like to thank Prof Dr Adnan Derdiyok for his valuable discussions and RA Abdullah Başçi for his help and implementation.

## References

[1] T. Das, I.N. Kar, "Design and implementation of an adaptive fuzzy logic-based controller for wheeled mobile robots", IEEE Transactions on Control Systems Technology, Vol. 14, pp. 501–510, 2006.

[2] R. Carelli, J. Santos-Victor, F. Roberti, S. Tosetti, "Direct visual tracking control of remote cellular robots", Robotics and Autonomous Systems, Vol. 54, pp. 805–814, 2006.

[3] S. Sun, "Designing approach on trajectory-tracking control of mobile robot", Robotics Computer-Integrated Manufacturing, Vol. 21, pp. 81–85, 2005.

[4] M. Hsiao, C. Chen, S. Tsai, S. Liu, "Combined interval type-2 fuzzy kinematic and dynamic controls of the wheeled mobile robot with adaptive sliding-mode technique", IEEE International Conference on Fuzzy Systems, pp. 20–24, 2009.

[5] R. Sepúlveda, O. Castillo, P. Melin, A. Rodríguez-Díaz, O. Montiel, "Experimental study of intelligent controllers under uncertainty using type-1 and type-2 fuzzy logic", Information Sciences, Vol. 177, pp. 2023–2048, 2007.

[6] W.S. Lin, C.L. Huang, M.K. Chuang, "Hierarchical fuzzy control for autonomous navigation of wheeled robots", IEE Proceedings: Control Theory and Applications, Vol. 152, pp. 598–606, 2005.

[7] Z. Hendzel, M. Szuster, "Discrete neural dynamic programming in wheeled mobile robot control", Communications in Nonlinear Science and Numerical Simulation, Vol. 16, pp. 2355–2362, 2011.

[8] K. Su, Y. Chen, S. Su, "Design of neural-fuzzy-based controller for two autonomously driven wheeled robot", Neurocomputing, Vol. 73, pp. 2478–2488, 2010.

[9] T. Das, I.N. Kar, S. Chaudhury, "Simple neuron-based adaptive controller for a nonholonomic mobile robot including actuator dynamics", Neurocomputing, Vol. 69, pp. 2140–2151, 2006.

[10] G. Oriolo, A. De Luca, M. Vendittelli, "WMR control via dynamic feedback linearization: design implementation, and experimental validation", IEEE Transactions on Control Systems Technology, Vol. 10, pp. 835–852, 2002.

[11] J. Zhong Ping, N. Henk, "Tracking control of mobile robot: a case study in backstepping", Automatica, Vol. 33, pp. 1393–1399, 1997.

[12] W.G. Wu, H.T. Chen, Y.J. Wang, "Global trajectory tracking control of mobile robots", Acta Automatica Sinica, Vol. 27, pp. 326–331, 2001.

[13] F. Pourboghrat, M.P. Karlsson, "Adaptive control of dynamic mobile robots with nonholonomic constraints", Computers and Electrical Engineering, Vol. 28, pp. 241–253, 2002.

[14] T. Das, I.N. Kar, "Design and implementation of an adaptive fuzzy logic-based controller for wheeled mobile robots", IEEE Transactions on Control Systems Technology, Vol. 14, pp. 501–510, 2006.

[15] F. Martins, W.C. Celeste, R. Carelli, M. Sarcinelli-Filho, T. Bastos-Filho "An adaptive dynamic controller for autonomous mobile robot trajectory tracking", Control Engineering Practice, Vol. 16, pp. 1354–1363, 2008.

[16] J. Keighobadi, Y. Mohamadi, "Fuzzy sliding mode control of non-holonomic wheeled mobile robot", 9th IEEE International Symposium on Applied Machine Intelligence and Informatics, 2011.

[17] C.Y. Chen, T.H.S. Li, Y.C. Yeh, "EP-based kinematic control and adaptive fuzzy sliding-mode dynamic control for wheeled mobile robots", Information Sciences, Vol. 179, pp. 180–195, 2009.

[18] J.J.E. Slotine, W. Li, Applied Nonlinear Control, New Jersey, Prentice-Hall, 1991.

[19] K.D. Young, V.I. Utkin, U. Ozguner, "A control engineer's guide to sliding mode control", IEEE Transactions on Control Systems, Vol. 7, pp. 328–342, 1999.

[20] M. Dal, R. Teodorescu, "Sliding mode controller gain adaptation and chattering reduction techniques for DSP-based PM DC motor drives", Turkish Journal of Electrical Engineering & Computer Sciences, Vol. 19, pp. 531–549, 2011.

[21] K. Jezernik, M. Rodic, R. Safaric, B. Curk, "Neural network sliding mode robot control", Robotica, Vol. 15, pp. 23–30, 1997.

[22] M. Ertuğrul, A. Şabanoviç, O. Kaynak, "Various VSS techniques on the control of automated guided vehicles", Marmara Research Center, Technical Report, 1994.